

## InAs/GaSb superlattice interband cascade light emitting diodes with high output power and high wall-plug efficiency

Yi Zhou <sup>a</sup>, Qi Lu <sup>b</sup>, Xuliang Chai <sup>a,c</sup>, Zhicheng Xu <sup>a</sup>, Jianxin Chen <sup>a,\*</sup>, Anthony Krier <sup>b</sup>, Li He <sup>a</sup><sup>a</sup> *Key Laboratory of Infrared Imaging Materials and Detector, Shanghai Institute of Technical Physics, Chinese Academy of Science, Shanghai 200083, China*<sup>b</sup> *Physics Department, Lancaster University, Lancaster, LA1 4YB, United Kingdom*<sup>c</sup> *University of Chinese Academy of Sciences, Beijing 100049, China*

## Abstract:

In this work, 2-stage and 5-stage mid-infrared superlattice interband cascade light emitting diodes (ICLEDs) were fabricated and studied at different temperatures. The ICLEDs were composed of InAs/GaAsSb active regions, InAs/AlAsSb injection regions and GaAsSb/AlAsSb tunneling regions. The devices exhibited high output power and very low series resistance, indicating efficient carrier blocking and tunneling in the designed structure. Radiances of 0.73 W/cm<sup>2</sup>-sr and 0.38 W/cm<sup>2</sup>-sr were achieved at 300K for the 5-stages and the 2-stages ICLEDs, respectively. With an output power of 3.56 mW, the wall-plug efficiency of the 5-stage ICLED reached 0.5% at 80 K, under 350 mA injection current. The efficiency was largely maintained in the same range with increasing current injection. The results showed that ICLEDs have great potential for mid-infrared LED applications requiring large output power and high wall-plug efficiency.

## Key words:

Superlattice, interband cascade LED, high wall-plug efficiency

The interband cascade structures were first developed and used in lasers by Yang.<sup>1,2</sup> Interband cascade lasers (ICLs) can produce coherent radiation over a large part of the mid-infrared spectral range.<sup>3,4</sup> The use of interband transitions in the cascade devices allowed the ICLs to work at lower electrical input powers than quantum cascade lasers. Besides, the interband cascade photovoltaic devices were also proposed by Yang in 2010 and have been successful in their application to infrared photodetectors and thermophotovoltaic (TPV) devices.<sup>5-9</sup> Recently, more investigations have been carried out on the application of interband cascade structures in mid-infrared LEDs with high output power and wall-plug efficiencies (WPEs).<sup>10-13</sup> Various types of emitters have been utilized in the ICLED structures. Among them, the GaInAsSb quantum well (QW) based ICLEDs exhibited more than 6 mW output power at 77 K.<sup>10</sup> And the ICLEDs based on “W” structures achieved 2.9 mW output power at 300 K.<sup>11</sup> Both of these two types of ICLEDs emitted at relatively shorter wavelengths (~3.1 μm). For longer wavelengths emission, the InAs/GaSb superlattices (SLs) have been used more often. One of the key advantages of the InAs/GaSb superlattices is that the band structure can be tailored to suppress Auger recombination.<sup>14</sup> Because of the greatly reduced Auger recombination, which is the dominant non-radiative recombination mechanism in the high current injection regime, these superlattice materials are attractive as light emitters.<sup>15</sup> Ricker et al. demonstrated a 3.8 μm ICLED based on the InAs/GaSb SLs with 1.04 W/cm<sup>2</sup>-sr maximum radiance at 300 K.<sup>12</sup> A radiance of about 0.5 W/cm<sup>2</sup>-sr with 4.6 μm peak wavelength has also been reported from this type

of ICLEDs by Muhowski et al.<sup>13</sup> Table 1 below summarizes the room temperature performances of these different types of ICLEDs.

It can also be noticed from table 1 that the reported WPEs were still quite low. One reason is the low light extraction efficiency from these devices. Without any surface treatment or additional structures, only a few percent of the emitted photons can escape from the semiconductor/air interface due to the total internal reflections. In addition, the maximum value of the WPE typically occurred at low current injections. With increasing current, the efficiency quickly dropped to less than 0.1%. The high turn-on voltage of the ICLEDs in table 1 could be another reason for the low WPEs, especially under high injection currents. With 22 stages, the turn-on voltage of the ICLED by Kim et al. reached around 8 V at 300 K.<sup>11</sup> Despite with fewer stages, the GaInAsSb QW based ICLED still required a turn-on voltage of ~5 V.<sup>10</sup> In comparison, the InAs/GaSb SL based ICLEDs had relatively lower turn-on voltages (3-4 V).<sup>12, 13</sup> Researchers also examined the effects of a variety of tunnel junction designs for the SL based ICLEDs, trying to optimize the device structure and achieve higher WPE under high injection current. ICLEDs using AlInAsSb on the n-side of the tunnel junction had low turn-on voltage of 1.04 V from the 4-stage structure. However, the WPE for this structure still decreased quickly as injection current increased.<sup>16</sup>

Table 1. Performance comparison of different types of ICLEDs at 300 K.

| Work                                 | Emitter        | Number of stages | Turn-on voltage | Peak wavelength   | Maximum radiance                      | Maximum WPE |
|--------------------------------------|----------------|------------------|-----------------|-------------------|---------------------------------------|-------------|
| Ermolaev et al. (2018) <sup>10</sup> | GaInAsSb QWs   | 10               | ~5 V            | 3.1 $\mu\text{m}$ | 0.36 $\text{W}/\text{cm}^2\text{-sr}$ | ~0.18%      |
| Kim et al. (2018) <sup>11</sup>      | “W” structures | 22               | ~8 V            | 3.1 $\mu\text{m}$ | 0.73 $\text{W}/\text{cm}^2\text{-sr}$ | ~0.4%       |
| Ricker et al. (2017) <sup>12</sup>   | InAs/GaSb SLs  | 8                | ~3 V            | 3.8 $\mu\text{m}$ | 1.04 $\text{W}/\text{cm}^2\text{-sr}$ | ~0.4%       |
| Muhowski et al. (2017) <sup>13</sup> | InAs/GaSb SLs  | 16               | ~4 V            | 4.6 $\mu\text{m}$ | ~0.5 $\text{W}/\text{cm}^2\text{-sr}$ | -           |

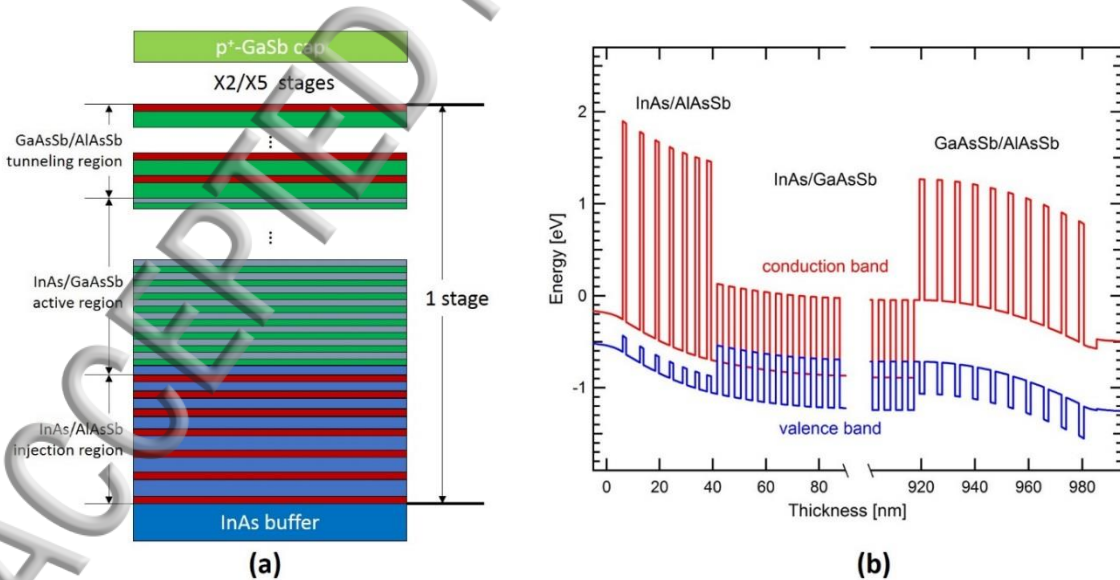


Figure 1. (a) Schematic illustration of the ICLED structure. (b) Calculated band alignments of one stage of the ICLED under forward bias.

In this paper, we present the results of MWIR 2-stage and 5-stage ICLEDs based on the InAs/GaSb SLs. The emission regions, which are similar to the absorption regions in the interband cascade infrared photodetectors (ICIPs),<sup>5,6</sup> were inserted between the InAs/AlAsSb electron injection region and the GaAsSb/AlAsSb tunneling region. Both regions also act as hole and electron barriers. The barriers can prevent carriers from leaking from one emission region to the next without recombining radiatively. The ICLED structure is illustrated in Fig. 1(a). The whole device structure was quite similar to the ICIP except that the ICLED worked under forward bias and the device should remain low in series resistance for current recycling to achieve high WPE. These ICLEDs can also work as photodetectors or TPVs under reverse bias or zero bias.

The ICLEDs for this work were grown on n-type InAs (100) substrates by solid-source MBE. The ICLED structure consists of a 1  $\mu\text{m}$  Si-doped ( $n=1\times 10^{18}/\text{cm}^3$ ) InAs buffer layer, followed by a sandwich cascade structure, including a Si-doped ( $n=1.5\times 10^{17}/\text{cm}^3$ ) electron injection region consisting of 7 InAs/AlAsSb quantum wells to form energy steps, a 0.8  $\mu\text{m}$  light Be-doped ( $n=5\times 10^{15}/\text{cm}^3$ ) 8ML InAs/7ML GaAsSb emission region and 10 periods of Be-doped ( $n=1\times 10^{17}/\text{cm}^3$ ) 16ML GaAsSb/6ML AlAsSb p-type superlattice as a tunneling region. The 2-stage ICLED repeats the cascade structure twice and the 5-stage ICLED repeats it 5 times. They were both topped with a thin Be-doped ( $n=1\times 10^{18}/\text{cm}^3$ ) GaSb contact layer. The band alignments of one stage under forward bias were calculated using *Nextnano*, as shown in Fig. 1(b). Both two samples were grown at 480°C which is higher than GaSb based structures, providing low defect density and high quality materials.<sup>17</sup> The lattice mismatch to InAs substrates is less than  $3.0\times 10^{-5}$ , the full width half maxima (FWHM) of 1<sup>st</sup> satellite peak in XRD rocking curve is less than 24", and the rms surface roughness is  $< 0.5$  nm over an area of 10  $\mu\text{m}\times 10$   $\mu\text{m}$ , indicating excellent lattice quality and high uniformity, similar to the results of the ICIP shown in our previous work.<sup>18</sup> All the samples were processed into single element devices with different sizes, using standard wet etching techniques without passivation. The processed devices were then mounted onto TO headers for optical and electrical characterization in an Oxford Instrument liquid helium cooled cryostat, which can provide temperatures from 6 K to 300 K. Emission spectra were measured with a Bruker Vertex fourier transform infrared (FTIR) spectrometer utilizing a double-modulation scheme, and an external 77 K InSb photodiode detector. Light-current-voltage (LIV) curves were recorded by injecting currents pulses into a mesa diode from 20 mA to 1600 mA. Emitted power was recorded with an integrating sphere system and a calibrated PbSe amplified photodetector for the devices under test.

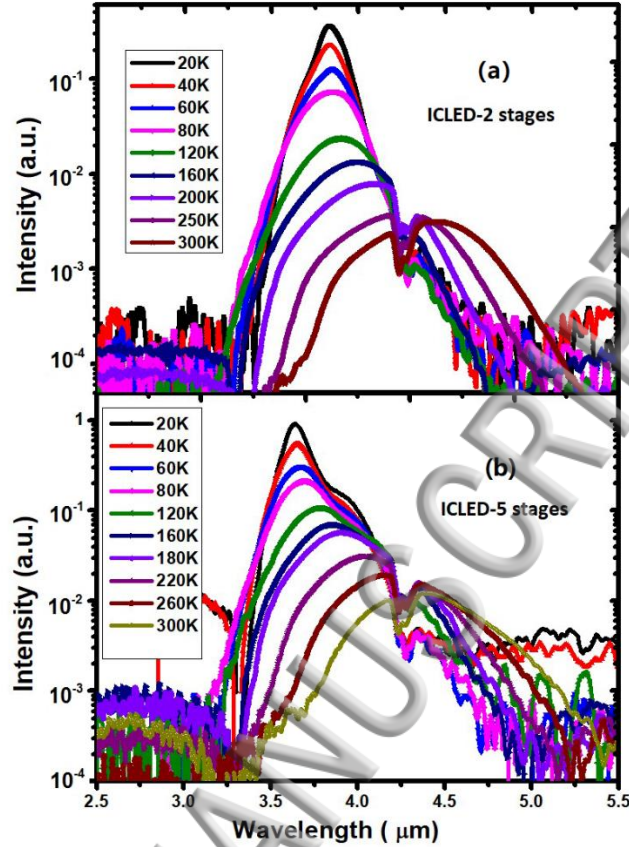


Figure 2. Electro-luminescence spectra from the 2-stage (a) and 5-stage ICLEDs (b) measured from 20 K to 300 K with 100 mA current injection.

The electroluminescence emission spectra of both the 2-stage and 5-stage ICLEDs at various temperatures shown in Fig. 2 using an injection current of 100 mA for both devices. The emission peaked at 3.83  $\mu\text{m}$  and 3.64  $\mu\text{m}$  at 20 K for the 2-stage and 5-stage ICLEDs, then red-shifted to 4.47  $\mu\text{m}$  and 4.39  $\mu\text{m}$  at 300K respectively, largely due to bandgap narrowing of the materials. The emission spectra of the 2-stage ICLED had a full-width at half-maximum (FWHM) of 174 nm at 20 K, which broadened to 733 nm at 300 K. While for the 5-stage ICLED, a similar FWHM of 153 nm was measured at 20 K, broadening to 710 nm at 300 K. The peak intensity dropped by nearly two orders of magnitude with increasing temperature from 20 K to 300 K, and the integrated intensity became about 30 times weaker, largely due to the competing nonradiative Auger recombination at higher temperatures. However, it is worth pointing out that the quenching of our device was clearly slower than the LEDs based on InAsSb bulk material and InAs/InAsSb quantum wells.<sup>19,20</sup> From the theoretical study, it was found out that the Auger rate in the InAs/GaSb SLs had much weaker temperature dependence than the bulk materials,<sup>21</sup> contributing to the slower reduction of the EL intensity with rising temperature. At 77 K, the Auger rate of the InAs/GaSb SLs is in the order of  $10^{-28}$   $\text{cm}^6/\text{s}$ , much smaller than the narrow bandgap bulk materials and InAs/InAsSb SLs ( $\sim 1 \times 10^{-26}$   $\text{cm}^6/\text{s}$ ),<sup>14</sup> making the InAs/GaSb SL a superior emitter in the mid-infrared range. As mentioned earlier, the ICLED can also be used as a photodetector, so we also measured the photo-response curves of the 5 stage interband device under zero bias from 90 K to 300 K. The emission peaks of the ICLED coincided well with the 50% cutoff wavelength of the same device working as photodetector under 0 bias, as shown in Fig 3. The electric performance and detectivity was measured in a similar manner to the ICIP results reported in our previous work.<sup>18</sup>

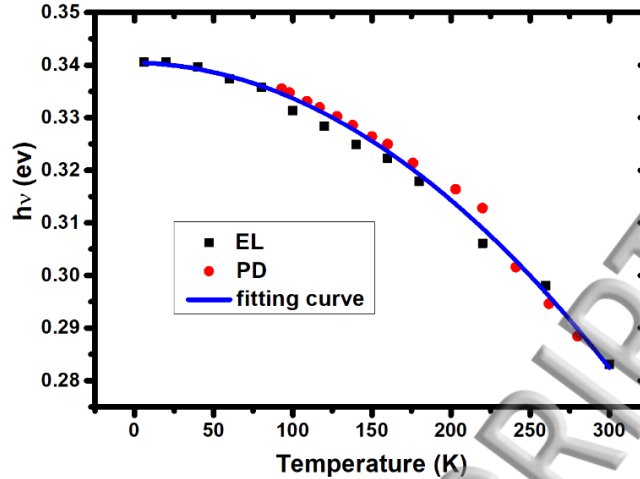


Figure 3. Temperature dependence of the band gap measured by the electroluminescence (EL), compared with the result of photodetector (PD) (red dot), as well as the fitting curve (blue line).

Figure 4 illustrates the dependence of radiance and external quantum efficiency on input current density at 300 K for both ICLEDs with different mesa sizes, providing an explanation of the observed power scaling with mesa dimensions. Firstly, the emitted power was recorded with an integrating sphere system, then the radiance data was calculated by assuming the light emission from these devices have Lambertian light distribution pattern. The maximum radiance of 0.73 W/cm<sup>2</sup>-sr and 0.38 W/cm<sup>2</sup>-sr were achieved from the 5-stage and 2-stage ICLEDs respectively, with the smallest mesa (200 × 200 μm) under the maximum injection current of 1600 mA. The curves for different diameter mesas made from the same type of ICLED were coincident, indicating that similar limiting factors determined the behavior with little size dependence under our test conditions. The maximum radiance of the 5-stage ICLED was nearly twice that of the 2-stage one, indicating that adding more stages can result in higher emitted power using the same input current density, due to the carrier cascading nature of the ICLEDs. Nearly complete saturation of the output power density was observed for the two ICLEDs with the smallest sizes at high current injection, possibly due to the higher carrier leakage and stronger Auger recombination at large bias. As the packaging of the device was not optimized, 1% duty cycle at 1 kHz was used to minimize the effects of Joule heating. The thermal loading due to the TO-packaging imposed limitations to device performance, indicating that the thermal management and packaging of ICLEDs is very important for future applications.

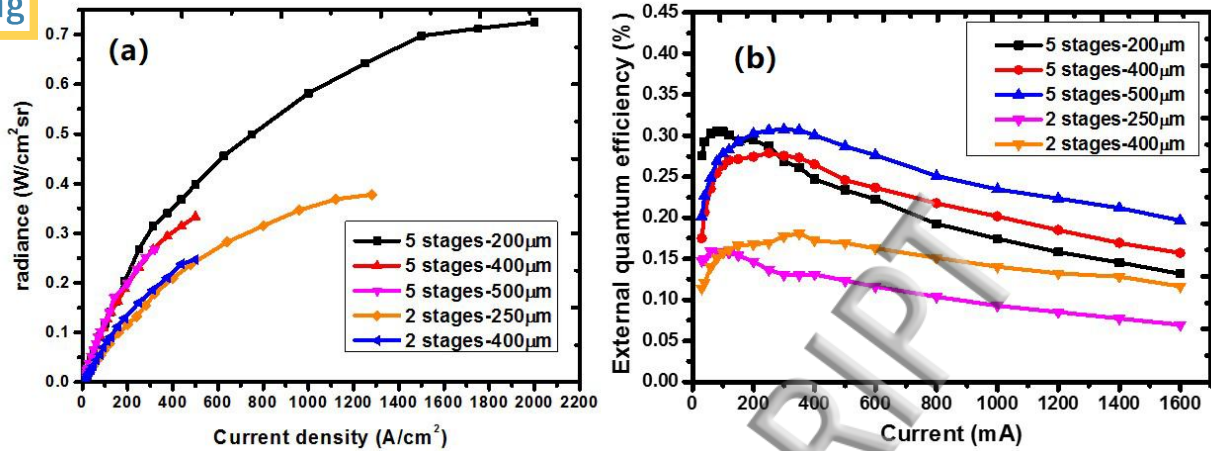


Figure 4. (a) Radiance and (b) external quantum efficiency of the 2-stage and 5-stage ICLEDs of various mesa diameter vs current density at room temperature.

Current–voltage (I-V) characteristics of the two devices at temperatures from 20 K to 300 K are shown in Fig. 5. The current in both devices turned on at reasonably low voltages. The 5-stage ICLED had a larger turn-on voltage because of the extra stages. The turn-on voltage was measured to be approximately 0.8 V and 1.6 V for the 2-stage and 5-stage ICLEDs respectively, at 20 K, which then reduced to around 0.2 V at 300 K. The dynamic resistances dropped quickly with increasing bias and was measured to be only  $\sim 1.5 \Omega$  for both 2-stage and 5-stage devices at 300 K. The low dynamic resistance effectively helps to reduce energy loss through Joule heating, also indicating that the band alignments of the injection region and the tunneling region were optimized so that the carriers experienced little obstacle in moving in the desired directions.

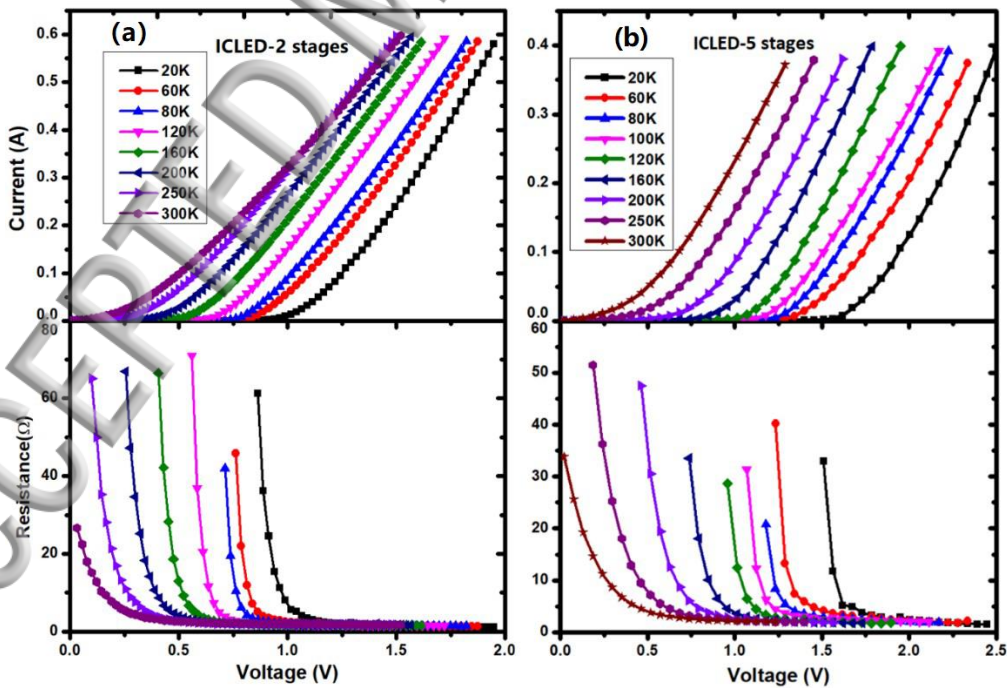


Figure 5. Forward bias I-V curves and dynamic resistance of (a) 2-stage and (b) 5-stage ICLEDs from 20 K to 300 K.

However, low series resistance alone is not enough for a high quality LED. Holes also should be effectively confined in each stage, to prevent them from passing through the active region without emitting photons. The emitted power of the 5-stage ICLED with a mesa size of  $400 \times 400 \mu\text{m}$  was recorded at 300 K. The emitted power at other temperatures were calculated from the result at 300 K and the normalized emission spectra at different temperatures. The output power increased with injection current at all temperatures as shown in Fig. 6. It was measured to be 5.96 mW at 20 K using an injection current of 300 mA. The high output power under high injection current indicates that the electron injection region of the InAs/AlSb multiple quantum wells worked well as a hole blocking layer, preventing the injected holes from passing through the active region without producing radiative recombination.

The WPEs were calculated by dividing the total output power by the input power, which decreased as temperatures increased due to Auger recombination. At 20 K, the WPE was estimated to be around 1.4% from 20 mA to 150 mA. The low efficiency is predominantly caused by the low extraction efficiency which was limited by the total internal reflection at the semiconductor-air interface. Our devices were surface-emitting through a GaSb cap layer, so that the critical angle was only  $15.3^\circ$ . The collected (upper) emission of the ICLED is limited to about 1.8% of the total emission.<sup>17</sup> This is also one of the key reasons for the low maximum WPEs reported in Table 1. In addition, almost all the previously published works on ICLEDs showed a quick reduction of WPEs with increasing current. For example, at 300 K the WPE of the  $3.1 \mu\text{m}$  QW based ICLED ( $\sim 500 \mu\text{m}$  diameter) decreased from 0.2% to about 0.1% at 350 mA, and further down to  $\sim 0.07\%$  at 580 mA.<sup>10</sup> At 77 K, the  $3.7 \mu\text{m}$  SL based ICLED ( $520 \times 520 \mu\text{m}^2$  size) exhibited maximum WPE of 0.9%, which decreased to about 0.4% at 350 mA current injection.<sup>22</sup> With nearly the same emission wavelength as our device, the 16-stage ICLED ( $24 \times 24 \mu\text{m}^2$  size) by Muhowski et al. showed that the WPE decreased from 0.1% to 0.05% by increasing current at 77 K.<sup>13</sup> In comparison, at 20 K the WPE of our 5-stage ICLED only decreased from 1.4% at 20 mA to 0.9% at 300 mA. At 80 K, the WPE value dropped from 0.7% to 0.5% at 350 mA, which was about 10 times higher than the value reported by Muhowski et al., and slightly better than the  $3.7 \mu\text{m}$  ICLED by Keorperick et al. At 300 K, the WPE was reduced from 0.14% at 20 mA to 0.06% at 350 mA. Up to date, very little has been reported on the room temperature WPEs from ICLEDs emitting above  $4 \mu\text{m}$  wavelength. It is also worth noting that the size of the devices would also affect the dependence of the WPE on injection current density.<sup>22</sup> Our device size was ( $400 \times 400 \mu\text{m}^2$  size) close to those of Ermolaev et al. and Keorperick et al. A direct comparison of devices with the same size would be favored in the future.

In addition, our ICLED only had 5 stages, by using more stages, the external quantum efficiency can increase in proportion, as is shown in Fig. 4(b), thus achieving much higher output power. However, the WPE is likely to stay nearly constant by adding more stages in the structure, due to the increase of the turn on voltage. In our device, the InAs/GaSb SL emitter region was about 800 nm thick in each stage, which was much thicker than in the previously reported works.<sup>12,13</sup> By reducing the thickness of the emitter region in the future work, the series resistance will possibly further decrease, and the MBE growth duration can be significantly cut down. Our results also indicated that the InAs/AlSb multiple quantum wells can give good hole confinement even under high injection current, along with very low series resistance to avoid power loss. The output power of our ICLEDs did not show saturation at 350 mA, due to that 1% duty circle for the current was used to minimize the thermal heating. These devices were mounted on TO headers without any efficient cooling. Epi-side-down techniques with backside emitting configuration could possibly be used for device packaging so that they can work efficiently with 50% duty circle or DC current.<sup>23</sup> Additional micro-structured patterns could also be added onto the emitting surface to overcome the light extraction limit.<sup>24</sup>

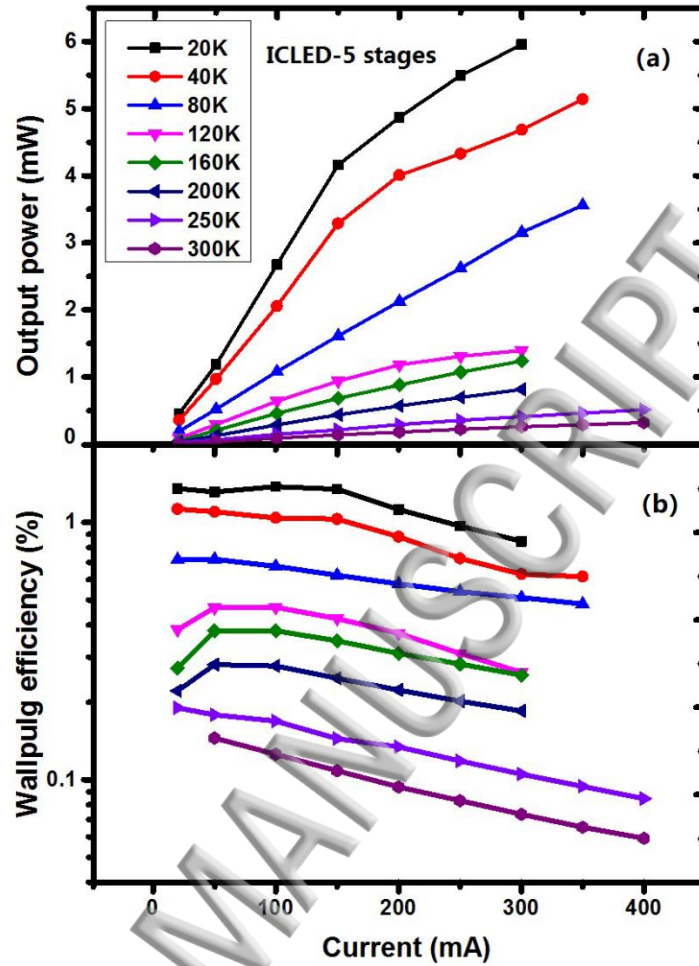


Figure 6. Output power (a) and WPE dependence on current injection (b) at 20-300 K for the 5-stage ICLED with a mesa size of  $400 \times 400 \mu\text{m}$ .

#### Conclusion:

In this study we have demonstrated bright electroluminescence from MWIR InAs/GaSb superlattice ICLEDs. The devices exhibited low turn-on voltage and low series resistance, which originated from the optimized tunneling region and injection region. The results also indicated that the InAs/AlAsSb electron injection region provided a sufficient barrier for hole confinement within the active region. Radiance of  $0.73 \text{ W/cm}^2\text{-sr}$  and  $0.38 \text{ W/cm}^2\text{-sr}$  were achieved at 300K for the 5-stages and the 2-stages ICLEDs, respectively. The WPE of the 5-stage ICLED was measured to be 0.9% at 20 K at 300 mA, and 0.5% at 80 K at 350 mA, much higher than previously reported values from similar structures. The output power reached 5.96 mW and 3.56 mW at 20 K and 80 K respectively. Contrary to the drastic decline of the WPE with increasing current observed in previous work, the WPE of our ICLEDs showed much less dependence on current injection, benefiting from the efficient carrier tunneling and blockage. The results demonstrated that the ICLEDs have great potential in MWIR LED applications requiring high brightness and high WPE.



## Acknowledgement:

This work was supported by the National Key Research and Development Program of China (Grant No. of 2016YFB0402403), the EPSRC grant of UK (No.: EP/P012035/1), the National Natural Science Foundation of China (NSFC) (Grant Nos. of 61534006, 61505237, 61505235, 61404148, 61176082) and the Youth Innovation Promotion Association, CAS (Grant No. 2016219). The underlying data in this paper is available from <http://dx.doi.org/10.17635/XXXXXXX>.

## Reference

- [1] R.Q. Yang, Superlattices Microstruct. 17, 77-83 (1995).
- [2] R.Q. Yang, S.S. Pei, J. Appl. Phys. 79, 8197 (1996).
- [3] L. Li, Y. Jiang, H. Ye, R.Q. Yang, T.D. Mishima, M.B. Santos, M.B. Johnson, Appl. Phys. Lett. 106, 251102 (2015).
- [4] L. Li, Z. Tian, Y. Jiang, H. Ye, R.Q. Yang, T.D. Mishima, M.B. Santos, M.B. Johnson, Conference on Lasers and Electro-Optics (CLEO), CF3K.2. (2012).
- [5] R.Q. Yang, Z. Tian, Z. Cai, J.F. Klem, M.B. Johnson, H.C. Liu, J. Appl. Phys. 107, 054514 (2010).
- [6] L. Lei, L. Li, W. Huang, J.A. Massengale, H. Ye, H. Lotfi, R. Q. Yang, T. D. Mishima, M. B. Santos, M. B. Johnson, Appl. Phys. Lett. 111, 113504 (2017).
- [7] H. Lotfi, L. Li, L. Lei, Y. Jiang, R.Q. Yang, J.F. Klem, M.B. Johnson, J. Appl. Phys. 119 023105 (2016).
- [8] H. Lotfi, L. Li, H. Ye, R.T. Hinkey, L. Lei, R. Q. Yang, J.C. Keay, T.D. Mishima, M.B. Santos, M.B. Johnson, Infrared Phys. Technol. 70, 162–167 (2015).
- [9] H. Lotfi, L. Li, L. Lei, R.Q. Yang, J.F. Klem, M.B. Johnson, IEEE J. Photovolt. 7, 1462-8 ( 2017).
- [10] M. Ermolaev, Y. Lin, L. Shterengas, T. Hosoda, G. Kipshidze, S. Suchalkin, G. Belenky, IEEE Photonic Tech. L. 30, 869-872 (2017).
- [11] C.S. Kim, M. Kim, W.W. Bewley, C.D. Merritt, C.L. Canedy, M.V. Warren, I. Vurgaftman, J.R. Meyer, Proc. of SPIE 10540, 1054009 (2018).
- [12] R.J. Ricker, S.R. Provence, D.T. Norton, T.F. Boggess, J.P. Prineas, J. Appl. Phys. 121, 185701 (2017).
- [13] A.J. Muhowski, R.J. Ricker, T.F. Boggess, J.P. Prineas, Appl. Phys. Lett. 111, 243509 (2017).
- [14] J.P. Prineas, R.J. Ricker, A. Muhowski, C. Bogh, S.R. Provence, T.F. Boggess, Proc. of SPIE 10124, 101240K (2017).
- [15] C.H. Grein, M.E. Flatt, J.T. Olesberg, S.A. Anson, L. Zhang, T.F. Boggess, J. Appl. Phys. 92, 7311 (2002).
- [16] L.M. Murray, D.T. Norton, J.T. Olesberg, T.F. Boggess, J.P. Prineas, J. Vac. Sci. Technol. B 30, 021203 (2012).

- [17] F. Wang, J. Chen, Z. Xu, Y. Zhou, L. He, *Opt. Express* 25, 1629 (2017).
- [18] Y. Zhou, J. Chen, Z. Xu, L. He, *Semicond. Sci. Technol.* 31 085005 (2016).
- [19] A. Krier, H.H. Gao, V.V. Sherstnev, Y. Yakovlev, *J. Phys. D: Appl. Phys.* 32, 3117–3121 (1999).
- [20] P.J. Carrington, Q. Zhuang, M. Yin, A. Krier, *Semicond. Sci. Technol.* 24, 075001 (2009).
- [21] H. Mohseni, V.I. Litvinov, M. Razeghi, *Phys. Rev. B* 58, 15378-15380 (1998).
- [22] E.J. Koerperick, J.T. Olesberg, J.L. Hicks, J.P. Prineas, T.F. Boggess, *IEEE J. Quantum Electron.* 45, 849 (2009).
- [23] J. Abell, C.S. Kim, W.W. Bewley, C.D. Merritt, C.L. Canedy, I. Vurgaftman, J.R. Meyer, M. Kim, *Appl. Phys. Lett.* 104, 261103 (2014).
- [24] J.J. Wierer Jr, A. David, M.M. Megens, *Nat. Photon.* 3, 163–169 (2009).

